

Identifying auditory attention with ear-EEG: cEEGrid versus high-density cap-EEG comparison

This content has been downloaded from IOPscience. Please scroll down to see the full text.

2016 J. Neural Eng. 13 066004

(<http://iopscience.iop.org/1741-2552/13/6/066004>)

View [the table of contents for this issue](#), or go to the [journal homepage](#) for more

Download details:

This content was downloaded by: martinbleichner

IP Address: 134.106.150.180

This content was downloaded on 05/10/2016 at 14:30

Please note that [terms and conditions apply](#).

Identifying auditory attention with ear-EEG: cEEGrid versus high-density cap-EEG comparison

Martin G Bleichner^{1,2,4}, Bojana Mirkovic^{1,2} and Stefan Debener^{1,2,3}

¹Department of Psychology, Neuropsychology Lab, University of Oldenburg, Oldenburg, Germany

²Cluster of Excellence Hearing4all, Oldenburg, Germany

³Research Center Neurosensory Science, University of Oldenburg, Oldenburg, Germany

E-mail: martin.bleichner@uni-oldenburg.de

Received 26 April 2016, revised 7 August 2016

Accepted for publication 26 August 2016

Published 5 October 2016



CrossMark

Abstract

Objective. This study presents a direct comparison of a classical EEG cap setup with a new around-the-ear electrode array (cEEGrid) to gain a better understanding of the potential of ear-centered EEG. **Approach.** Concurrent EEG was recorded from a classical scalp EEG cap and two cEEGrids that were placed around the left and the right ear. Twenty participants performed a spatial auditory attention task in which three sound streams were presented simultaneously. The sound streams were three seconds long and differed in the direction of origin (front, left, right) and the number of beats (3, 4, 5 respectively), as well as the timbre and pitch. The participants had to attend to either the left or the right sound stream. **Main results.** We found clear attention modulated ERP effects reflecting the attended sound stream for both electrode setups, which agreed in morphology and effect size. A single-trial template matching classification showed that the direction of attention could be decoded significantly above chance (50%) for at least 16 out of 20 participants for both systems. The comparably high classification results of the single trial analysis underline the quality of the signal recorded with the cEEGrids. **Significance.** These findings are further evidence for the feasibility of around the-ear EEG recordings and demonstrate that well described ERPs can be measured. We conclude that concealed behind-the-ear EEG recordings can be an alternative to classical cap EEG acquisition for auditory attention monitoring.

Keywords: ear-EEG, cEEGrid, auditory attention, mobile EEG

(Some figures may appear in colour only in the online journal)

Introduction

Electroencephalography (EEG) is extensively used in neuroscience to study the brain–behavior relationship. EEG hardware is relatively low-priced and provides the

possibility to conduct mobile brain electrical activity recordings outside the classical lab environment (Debener *et al* 2012, de Vos and Debener 2013, Lin *et al* 2014). EEG studies ‘in the wild’ enable the study of brain function in complex, ecologically valid situations (Gramann 2011, 2014, Wascher *et al* 2014). Beyond helping to understand how the brain functions in everyday situations, mobile EEG can also be used for every day application such as brain–computer interfaces (De Vos *et al* 2014) and to address clinical needs, such as continuous EEG monitoring in epilepsy patients (Askamp and van Putten 2014). However, major limitations in this context are the need of electrode

⁴ Author to whom any correspondence should be addressed



Original content from this work may be used under the terms of the [Creative Commons Attribution 3.0 licence](https://creativecommons.org/licenses/by/3.0/). Any further distribution of this work must maintain attribution to the author(s) and the title of the work, journal citation and DOI.

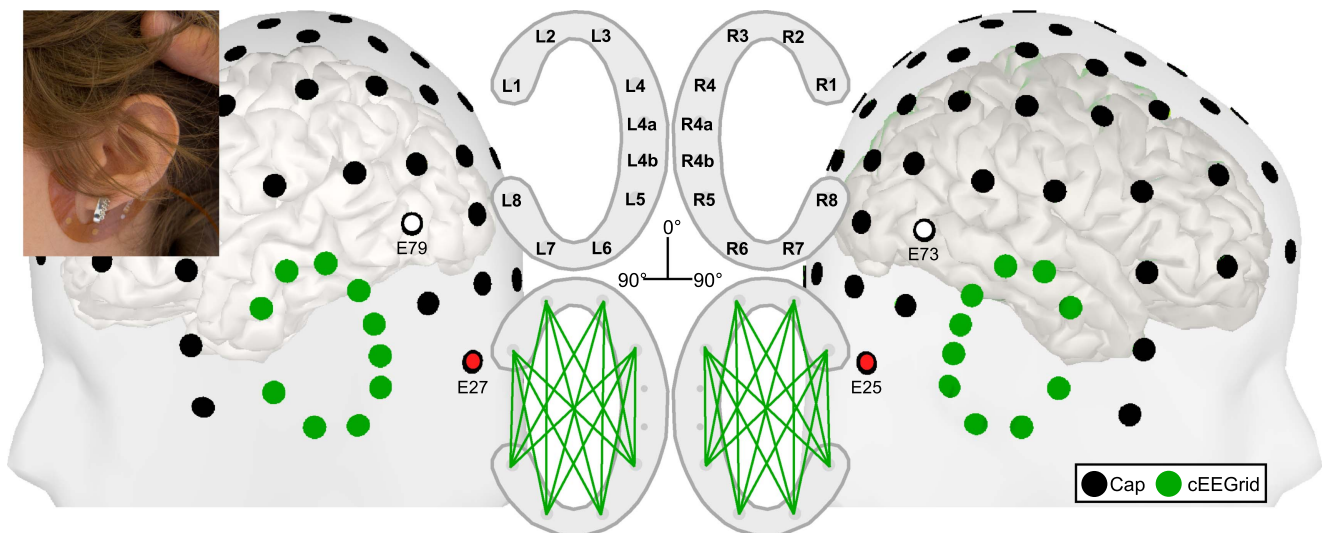


Figure 1. The digitized electrode positions of the cap-EEG (black) and cEEGrid (green) electrodes. The electrodes E27 and E25 (marked in red) were used as linked mastoid reference substitute for the cap, as no cap electrodes are located on the mastoids. Further bipolar derivations were computed between the electrodes E79 and E27, and the electrodes E73 and E25. The renderings were generated with the Brainstorm3 software. The cEEGrids are attached around the ear (inset upper left corner) with a double sided adhesive tape. The cEEGrids are designed as semi-disposable electrode grids. The flexprint material includes several layers of a biocompatible polyamide, the conductive parts consist of gold plated ends, pure copper traces, and conductive Ag/AgCl based polymer thick film ink. Middle: The electrode positions of the left and the right cEEGrid with the corresponding channel names. R4a and R4b serve as ground and reference during the recording. L4a and L4b are not considered in the analysis to keep the number of electrodes the same on both head sides. Below: The lines indicate the 32 bipolar channels that were used for the cEEGrid EEG classification. Center: Bipolar channels are considered to have an angle of 0° if the comprising electrodes are arranged vertically and 90° if they are arranged horizontally.

caps, and the clear visibility and poor comfort this technology comes with.

Classical head-mounted EEG caps are impractical for out-of-the-lab recordings and every day usage for several reasons. One is that they are not well accepted in public situations as they would raise attention of others (Askamp and van Putten 2014, Lee *et al* 2014). To solve this problem a number of ear-centered EEG systems have been proposed as an alternative that measure the EEG signal using miniaturized electrodes placed inside the outer ear-canal, the concha, or around the ear (Looney *et al* 2011, Lee *et al* 2014, Bleichner *et al* 2015, Debener *et al* 2015, Norton *et al* 2015). In-ear and around-the-ear electrodes can be worn comfortably and may not raise attention from others, that is, concealed use would be possible. Moreover, ear-centered EEG may interfere less with the participant's normal behavior and may not alter the behavior of other people around, hence it would be socially acceptable for every day usage. In combination with miniature wireless amplifiers and smartphone signal acquisition (Debener *et al* 2015) ear-centered EEG provides new opportunities for clinical as well as research-dedicated applications. Several studies have shown that ear-centered EEG can capture some of the signals that can be captured with classical scalp EEG very well. Obviously the location of ear electrodes, and the biased, smaller spatial coverage of the head sphere may make ear-centered EEG highly sensitive to some brain activity features and blind to others. However, due to the effects of volume conduction even far-field signals originating in remote cortical locations may be captured with

ear-centered EEG, as we and others have shown (Kidmose *et al* 2013, Bleichner *et al* 2015, Debener *et al* 2015).

Based on the results of a previous study (Bleichner *et al* 2015) we have developed a c-shaped multi-electrode array that is placed around the ear (cEEGrid; Debener *et al* 2015). The cEEGrids are designed as semi-disposable electrode grids. The flexprint material includes several layers of a biocompatible polyimide, the conductive parts consist of gold plated ends, pure copper traces, and conductive Ag/AgCl based polymer thick film ink. The ten electrodes are positioned around the ear using a double-sided adhesive tape (figure 1). A small amount of electrolyte electrode gel assures a low impedance electrode-skin contact. The conductive gel used to make the contact between cEEGrid electrodes and skin does not dry out over time as the electrode skin connection is sealed by the adhesive tape around the electrodes. We could show that the skin electrode contact is stable over the course of several hours, enabling the continuous recording of oscillatory as well as event-related potentials (Debener *et al* 2015).

The objective of the current study is to further evaluate the potential of the cEEGrid. Here we directly compare cEEGrid recorded EEG signals with concurrently recorded cap-EEG signals. Firstly, to see which ERP effects (and to what degree) of spatial auditory attention are detectable in the cEEGrid EEG in comparison to classical scalp EEG. Secondly, to evaluate whether single trial classification of spatial auditory attention is feasible using only the cEEGrid. Addressing these points is crucial to evaluate whether the cEEGrid, which allows for concealed EEG recordings, could

be an alternative to cap-EEG for auditory attention monitoring.

A paradigm developed by Choi *et al* (2013) was used, as it represents an approach that is potentially suitable for an auditory BCI application. Three auditory streams, which differ from each other in timbre, pitch progression, number of tones and sound direction, are presented simultaneously. The participants were asked to pay attention to one of the streams and to state whether the pitch progression was ascending, descending or alternating. These complex sound streams provide several cues for the listener to attend to, but they also provide a complex, challenging soundscape that requires the listener to pay attention to successfully complete the task. Choi *et al* (2013) showed that the temporal structure (i.e. onset of the tones) of the attended sound stream is reflected in the EEG trace and can be identified on a single-trial bases. We asked whether this finding can be confirmed in cEEGrid recordings. By directly comparing the simultaneously recorded cEEGrid and high-density scalp-EEG signals we were able to quantify the loss concealed EEG may come with the task of monitoring someone's auditory attention.

Methods

Participants

Twenty individuals participated in the study (mean age 25, 8 male, 1 left-handed) with self-reported normal hearing. The study was approved by the local ethics committee of the University of Oldenburg. All participants signed written informed consent prior to the experiment and were financially compensated for their participation.

Task

Participants performed an auditory attention task in which they had to shift their attention to one of several sound streams. Three concurrent sound streams were presented for three seconds. The streams differed in timbre (cello, oboe, and clarinet sound), sound direction (front, left, right) and number of tones (3, 4, and 5 respectively). Each stream was constructed of a sequence of tones that differed in pitch (for a detailed description of the construction of the tones please see Choi *et al* 2013). The tones were generated with Matlab (MATLAB R2012a, The Mathworks Inc. Natick, MA, USA) and had a sampling rate of 44 100 Hz. Each tone had a 100 ms cosine squared onset and offset ramp. The stream from the left side consisted of four tones (tone length 750 ms) which were based on a cello sound with a pitch of either 240 Hz or 300 Hz. The stream from the right side consisted of five tones (tone length 600 ms), the tones were based on an oboe sound with a pitch of either 720 or 900 Hz. The stream from the center consisted of three tones (tone length 1000 ms), the tones were based on a clarinet sound with a pitch of either 320 or 400 Hz. All three streams started simultaneously while the tone onsets of the remaining tones did not coincide in time. In each sequence the pitch changed either once or twice within

the trial, resulting either in an ascending, descending or alternating tone sequence. An ascending sequence started with a low pitch tone and ended with a high pitch tone after the pitch was changed once in between, a descending sequence started with a high pitch tone and ended with a low pitch tone after the pitch was changed once in between. The alternating sequence started and ended with the same tone pitch and the pitch was changed twice during the trial.

Listeners were instructed to pay either attention to the left or the right stream, but never the central stream. The side to be attended was cued by an arrow pointing either to the left or the right side, and listeners were instructed to indicate whether the attended sequence was ascending (press 8 on the numpad), descending (press 2) or alternating (press 5). In total 160 trials were presented. Participants were cued 80 times to pay attention to the left stream and 80 times to pay attention to the right stream.

Prior to the experiment participants had to fill in the Goldsmiths musical sophistication index (GOLD-MSI) to assess whether the musical background of the participants is related to task performance (Müllensiefen *et al* 2014, Schaal *et al* 2014).

Stimulus material and presentation

Stimulus presentation was controlled using the Psychophysics 3 toolbox for Matlab (Brainard 1997, Pelli 1997, Kleiner *et al* 2007). The sounds were presented binaurally in a soundproof booth at a comfortable listening level over EAR-Tone 3A insert earphones (3M Auditory Systems, Indianapolis, United States).

At the beginning of each trial a fixation point and an arrow indicating which stream had to be attended were presented in white on a black background on a computer screen distanced 1.3 m from the participant. The participants initiated each trial by pressing a button with their left hand, after which the arrow disappeared. The sound sequence started 1200 ms later, was presented for 3000 ms, and the participants had 1000 ms to give a response.

Procedure

After washing the hair and the skin around the ears the cEEGrid and the EEG cap were fitted. To each cEEGrid a double-sided sticky tape was attached and a drop of electrolyte gel was applied to each electrode (Abralylt HiCl, Easycap GmbH, Germany). The cEEGrids were positioned around the ears (figure 1, inset). Afterwards, the EEG caps were fitted. To each electrode the same electrolyte gel was applied and good impedance was assured for all electrodes (below 20 k Ω). After fitting of the cap the cEEGrids were connected with a wireless head-mounted amplifier (for details see below), which was attached with a headband at the back of the head. Electrodes from the EEG cap were attached to a second amplifier. During the recording, participants were seated in the sound shielded room in a comfortable chair.

The task took approximately 18 min, depending on how quickly the participant initiated the next trial. After

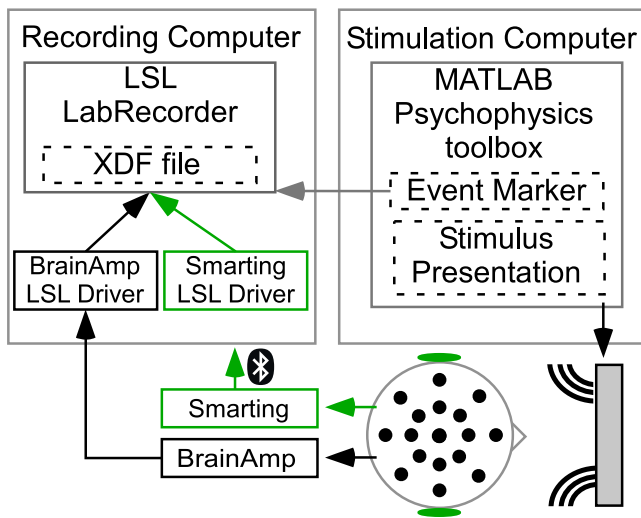


Figure 2. The stimulus presentation was controlled by the Psychophysics 3 MATLAB toolbox. The data of the two amplifiers and the event markers were synchronized and recorded using lab streaming layer (LSL LabRecorder App 1.05). The signal transmission between the Smarting amplifier and the recording computer was wireless using Bluetooth.

completion participants performed two other tasks which will be reported elsewhere. After EEG acquisition the exact positions of all cap and cEEGrid electrodes were digitized (Xensor electrode digitizer, ANT Neuro, The Netherlands).

Signal acquisition

We recorded EEG from scalp sites with a 96-channel Ag/AgCl EEG cap (Easycap, Hersching, Germany) with equidistantly placed electrodes with a central fronto-polar site as ground and the nose-tip as reference. From the 96-channels the channels around the ear that lay on top of the cEEGrid (6 at each side) had to be excluded, leaving 84-channel cap EEG data. The data were collected with a BrainAmp EEG amplifier system (BrainProducts, Gilching, Germany). From the around-the-ear sites we recorded from two 10 Ag/AgCl electrode cEEGrids. The electrodes R4a and R4b (figure 1, middle) were used as analog ground and reference, respectively. The position of the cap and grid electrodes is shown in figure 1. The cEEGrid data were collected with a customized SMARTING mobile amplifier (mBrainTrain, Belgrade, Serbia). For a detailed description of the cEEGrids and the amplifier used see (Debener *et al* 2015). The cEEGrid data were transmitted wirelessly to a recording computer via Bluetooth, while the cap data were transmitted via fiber optic cable from amplifier to a recording USB input box. Both systems used a sampling frequency of 500 Hz. The two EEG data streams and the stimulus triggers were combined and saved to a single file with the lab streaming layer (LSL) data acquisition and synchronization framework (<https://github.com/sccn/labstreaminglayer>) (The data was saved as .xdf file using the LSL LabRecorder software 1.05). See figure 2 for a

schematic of the recording setup. Due to signal buffering in the BrainAmp recording app there was a delay between the two EEG system streams and the trigger stream. This delay was quantified prior to the experiment for the complete setup. For this the audio output generated by the task was fed in simultaneously to both EEG systems and was recorded together with the triggers generated by the Psychophysics toolbox. This allowed us to quantify the timing delays of the two EEG streams and the stimulus triggers, the cEEGrid data ('cEEGrid-EEG' from here on) as recorded by the smarting amplifier was delayed by 38 ms, the scalp data ('cap-EEG' from here on) as recorded by the BrainAmp was delayed by 88 ms. The timing of all datasets were corrected accordingly.

Signal analysis

Pre-processing. EEG data were analyzed off-line using EEGLAB version 13.4.4b and custom scripts running under Matlab. The data from the cEEGrid and the cap were processed identically where possible and differently where necessary (see below). For the cap-EEG data an ICA based artefact attenuation was performed to correct for eye-blinks and eye movements. For this the raw EEG data was high-pass filtered at 1 Hz and low-pass filtered at 60 Hz and epoched into consecutive segments of 1000 ms. This segmentation was not related to the task structure and only used for the ICA procedure. Segments dominated by non-stereotypical artifacts were identified and rejected before ICA computation. The remaining data was then submitted to infomax ICA. The resulting ICA weights were applied to the original, unfiltered and un-epoched dataset.

Cap-EEG and cEEGrid-EEG data were high-pass filtered at 0.1 Hz and low-pass filtered at 10 Hz and down-sampled to 64 Hz. For the cap-EEG the ICA components were visually inspected and removed if they reflected eye movement related artefacts.

To allow for better comparability between the results of this study and the study of Choi *et al* (2013), the cap data were also referenced against the arithmetic mean of two electrodes that are located posterior to the mastoid position (E25 and E27, see figure 1). This location is not equivalent to the normal mastoid location but allows a better comparability with the previous results. If not otherwise stated the data remain referenced to the nose tip.

For the cEEGrid-EEG data all possible bipolar channel combinations per side (56 bipolar channels in total) were computed. For the comparison between the cEEGrid-EEG and the cap-EEG only the bipolar channels between the channels of the upper half of the grid (L1–L4 and R1–R4) and the lower half of the grid (L5–L8 and R5–R8), 32 channels in total, were used (see figure 1 for a visualization of the orientation of these bipolar channels). These channels should be most sensitive to the signal of interest as they may be aligned along the orientation of the tangential dipole explaining most variance in late AEPs (Nunez and Srinivasan 2006, Hine and Debener 2007).

Epoching. For ERP analysis and single trial classification, epochs from 0 to 3000 ms were extracted relative to the onset of the sound stream. The mean of the entire epoch was used for baseline correction. Epochs dominated by artifacts were identified using the probability criteria implemented in EEGLAB (standard deviation: 2) and rejected from further analysis. After removing these trials and the trials with incorrect responses, a minimum of 25% of the trials (for the participant with the worst task performance) and a maximum of 80% of the trials was available for analysis (mean 53%). The grand average ERP was computed for the attend-left and attend-right condition by averaging over all trials from one condition and consequently over all datasets.

ERP analysis. For the statistical analysis of the attend-left and attend-right ERP we performed a mass univariate analysis for all electrodes and all time points using a permutation test with 2500 permutations with a strong control of the family wise error rate (FWER) as described in (Groppe *et al* 2011) and implemented for EEGLAB (t_{\max} , Mass Univariate ERP Toolbox, http://openwetware.org/wiki/Mass_Univariate_ERP_Toolbox). For the cap data all electrodes and all time points between 0 and 3000 ms were included in the test. For the cEEGrid data all bipolar pairs with a vertical orientation (see above) and all time points between 0 and 3000 ms were included in the test. Additionally, we performed another permutation test for the cEEGrid data where we compared eight horizontally oriented channel pairs (L2–L3, L1–L4, L8–L5, L7–L6 and R2–R3, R1–R4, R8–R5, R7–R6) and eight vertically oriented channel pairs (L1–L8, L2–L7, L3–L6, L4–L5 and R1–R8, R2–R7, R3–R6, R4–R5) of the left and right cEEGrid, to get an estimate of the effect of the channel orientation on the signal of interest.

To analyze the attention effect on the single tone level (attended and unattended) we extracted sub-epochs from the trials that were used in the above analysis. For each tone (excluding the first one) an epoch was extracted from 0 to 600 ms relative to the single tone onsets. For the attend-left condition we extracted three epochs per trial corresponding to the last three notes of the left stream (attended notes) and four epochs corresponding to the last four notes of the right stream (unattended notes). For the attend-right condition we extracted four epochs corresponding to the last four notes of the right stream (attended notes) and the last three notes of the left stream (unattended notes). The attended tone of the attend-left and the attend-right condition were combined, as were the unattended tones. The grand average ERPs for attend-left and attend-right were computed. The effect size of attended versus unattended tones was measured as Hedges' g between 0 and 600 ms. Hedges' g is a variation of Cohen's d but reduces the estimation error for smaller samples by correcting the pooled variance. The interpretation of Hedges' g is analogous to Cohen's d , and effect size above 0.8 is considered as large. For the ERP analysis we computed the grand average over all trials and all dataset. This analysis was performed for three bipolar channels on the right hemisphere: cap vertex position minus E25 (figure 1, marked in red), cap

E73 minus cap E25, and cEEGrid R3 minus R6. The vertex channel pair allows a direct comparison of our results with the results from Choi *et al* (2013). The two other channel pairs allow a more direct comparison of the cap and the cEEGrid using electrodes at roughly the same location, inter-electrode distance, and orientation. Note that this cap pair is the best approximation for the cEEGrid pair we can achieve with our cap layout, but differences remain.

Single trial classification. For the single trial classification we used a leave-one-out cross validation template matching approach following the procedure described by (Choi *et al* 2013). For this an individual trial was compared with the average response of the remaining trials for the attend-left and the attend-right condition (i.e. attend-left and attend-right template). For each electrode the normalized cross-correlation function (NCF) was computed between each trial and the two templates. The cross-correlation was computed for the trial segment of 400–2800 ms, thereby excluding the onset response and the offset response. To allow for a small time jitter between the single trial and the template the maximal cross correlation in the range of -50 to 50 ms was determined. Consequently the difference between the maximum NCF for the left-template and the right-template was computed, and this value was summed up over all electrodes. A trial was classified as attend-left if the resulting value was positive (i.e. the match between trial and attend-left template is higher than between trial and attend-right template) and classified as attend-right otherwise. The classification accuracy is the number of correct classifications divided by the number of trials and the confusion matrix was computed for each participant. Further we computed for each participant whether the classification accuracy was significantly above the chance level using a binomial statistic with a confidence limit of $p = 0.05$, thereby taking the individual differences in the number of trials into account (Müller-Putz *et al* 2008). For the statistical analysis of the differences in classification accuracy and the behavioral response (hit rates) we used the non-parametric Friedman and Wilcoxon signed rank test. For these measures we provide the $r_{\text{equivalent}}$ as an effect size indicator (Rosenthal and Rubin 2003). The statistical analysis was performed using the statistical software package R (R Development Core Team 2013).

Inter-electrode distance and angle analysis. In ear-centered EEG the electrodes are arranged relatively close to each other. In order to gain a better understanding of the influence of the electrode distance and the orientation of the electrodes, we compared the single channel classification accuracy with the inter-electrode distance of the electrodes that comprise a bipolar channel and the orientation of these electrodes to each other. For each bipolar channel we computed the single channel classification accuracy and computed the distance between the two electrodes that comprise the bipolar channel as well as their respective angle. The distances were binned into six bins (1.9, 3.3, 3.8, 5.4, 5.9 and 6.9 cm). The angles

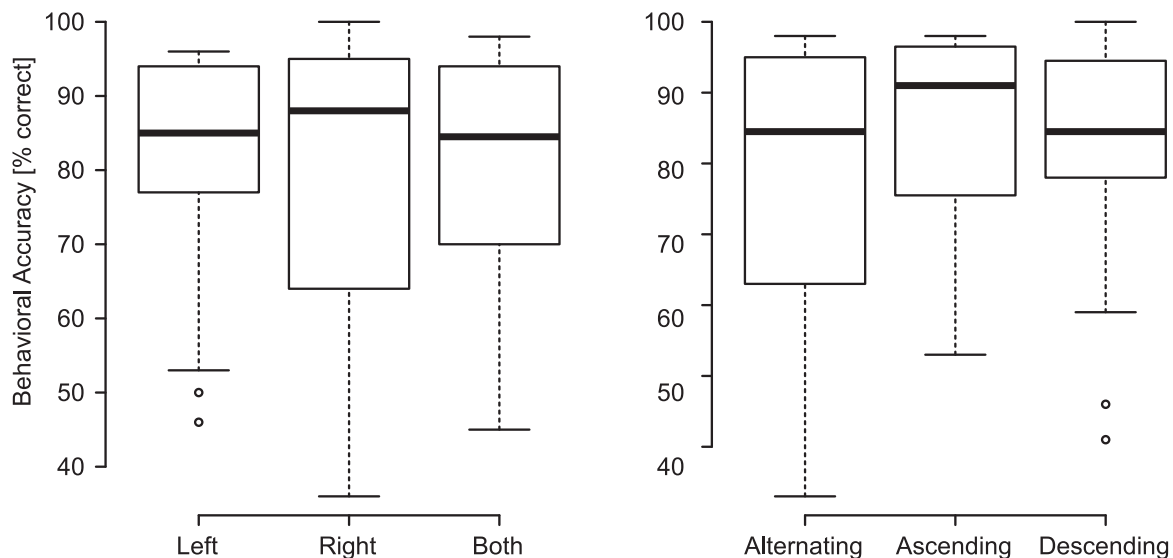


Figure 3. Behavioral responses shown for the stream direction (left) and the pitch progression (right), there were no significant differences in the response behavior for stream direction and pitch progression.

were computed as absolute values in respect to a vertical axis. The vertical axis was considered as 0° , the horizontal axis as 90° (see figure 1 middle). Note that, due to the ellipsoid shape of the cEEGrid the effects of bipolar channel distance and angle cannot be fully dissociated from each other.

Results

Behavioral results

Participants had to indicate for each attended tone sequence whether it was ascending, descending or alternating. On average participants responded in 84.5% (median hit rate) of the sequences correctly. The lowest performance was 45% the highest performance 98% correct responses (figure 3). The median in response accuracy for the attend-left condition was 85% and 88% for the attend-right condition. The Wilcoxon signed-rank test revealed that there was no significant difference between the two ($W = 1, Z = 0.8034, p = 0.4355, r_{\text{equivalent}} = 0.185$). The median response was 84% for alternating streams, 91% for ascending streams and 85% for descending streams. The Friedman test showed that there was no significant difference in hit rate for these different pitch progressions ($\chi^2(2) = 5.4805, p = 0.06455, r_{\text{equivalent}} = 0.858$). The overall high percentage of correct responses indicates that most of the participants could perform the task well. The error rate of 15% also indicates that the task was not too easy but that some effort had to be put into performing well. There was a positive correlation between the self-reported perception ability as measures by the MSI-Gold and the individual hit rate ($r = 0.51, p < 0.05$), indicating that people who judged themselves to be poor in musical perception performed worse in judging the tone sequences.

Attention modulation of the ERP

Figure 4(A) shows the grand average ERPs for the attend-left (blue) and the attend-right (red) condition for the cap-EEG (shown for the vertex electrode, referenced against the arithmetic mean of E25 and E27, see figure 1). In response to stimulus onset (i.e. the onset of all 3 streams) an auditory-evoked P1–N1–P2 complex is apparent in both conditions. For the attended tones (i.e. the subsequent tones) a comparable N1–P2 response is apparent for the attend-left and the attend-right condition. Compared to the response to stimulus onset, this response is reduced in amplitude and has a longer latency. The difference wave (figure 4(B), top) shows clear differences between the conditions especially in the second half of the stimulus. The permutation test reveals that the two conditions are significantly different at these later time points (figure 4(B), bottom). The raster diagram (figure 4(C)) illustrates the temporal–spatial distribution of the significant effects for each time–electrode bin (critical t -value: ± 5.55 , FWER corrected for multiple comparisons). The topographic representation (figure 4(D)) of the time bins with the strongest effect, show that the most significant differences are primarily at electrodes located over the left and right temporal cortex.

The grand average ERP for the cEEGrid (figure 5(A)) shows a clear evoked response (N1–P2 complex) to the stimulus onset and to the attended tones. The difference wave (figure 5(B) top) shows a difference between the conditions that increases over time. The permutation statistics shows that the two conditions are significantly different at these later time points (figure 5(B), bottom). The raster diagram (figure 5(C)) illustrates the temporal–spatial distribution of the significant effects for each time–electrode bin (critical t -value: ± 5.30 , FWER corrected for multiple comparisons). A direct comparison of vertically and horizontally oriented channel pairs of the cEEGrid (figure 5(D)) reveals significant differences between the conditions for the vertically but not

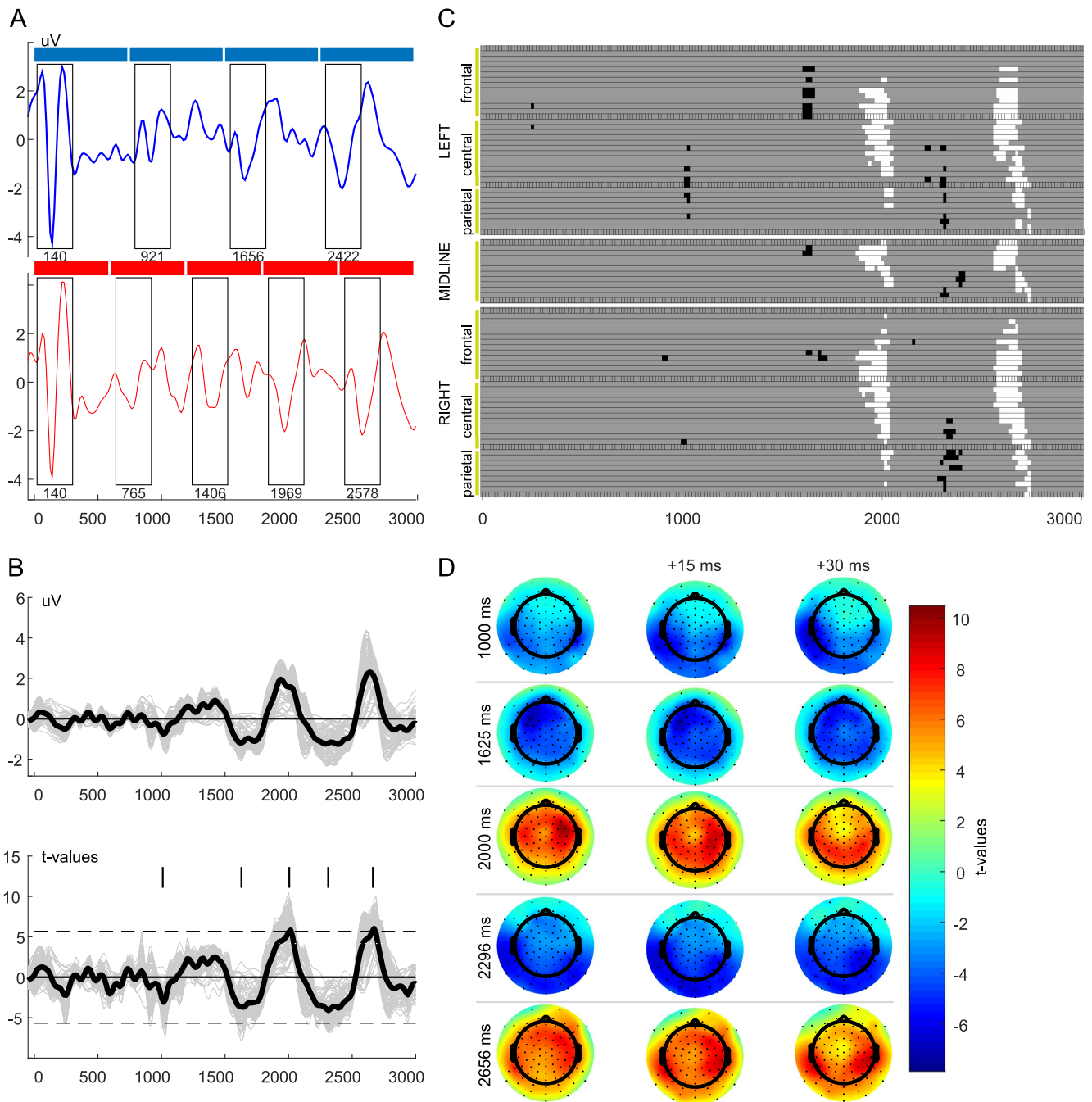


Figure 4. (A) Grand average ERP of one cap electrode (Vertex referenced to the arithmetic mean of E25 and E27) shown for the attend-left (blue) and attend-right (red) condition. The horizontal bars in blue (left sound stream) and red (right sound stream) indicate the sound onsets and sound durations. For each tone in the attended stream the onset responses can be seen (boxes), the numbers indicate the respective peak latencies. Based on the latency of the first N1 (140 ms) the peaks should occur at 890, 1630 and 2390 ms for the attend-left conditions, and at 740, 1340, 1940 and 2540 ms for the attend-right condition. The observed latencies occur approximately 35 ms later. (B) Top: butterfly plot illustrating difference waves between attend-left and attend-right condition. Each waveform (gray) represents one of the 84 cap electrodes. The black line shows the average difference wave for all electrodes. Bottom: butterfly plot of the temporal evolution of the t -values (attend left–attend right) for all cap electrodes (gray) and their average score (black) according to the permutation test. The horizontal dashed line represents the critical t -score (± 5.55 , FWER corrected for the number of channels and time points). A t -value more extreme than the critical t -score indicates a significant difference between the conditions for that electrode. The vertical lines indicate the time points for which the t -values exceed the critical t -value. (C) Raster diagram illustrating the same results for each electrode and time bin; each row represents one electrode, each column represents one time bin. White and black rectangles indicate electrodes/time points in which the ERP differences are significant, more positive or negative respectively. Gray rectangles indicate electrodes/time points at which no significant differences were found. The electrodes are arranged roughly topographically along the y-axis. (D) Topographic representation of the t -values shown for five time points (that showed above threshold t -values of ± 5.55 , see vertical lines in plot (B) and the respective two successive time points). The significant electrodes are located primarily over the left and right temporal lobes.

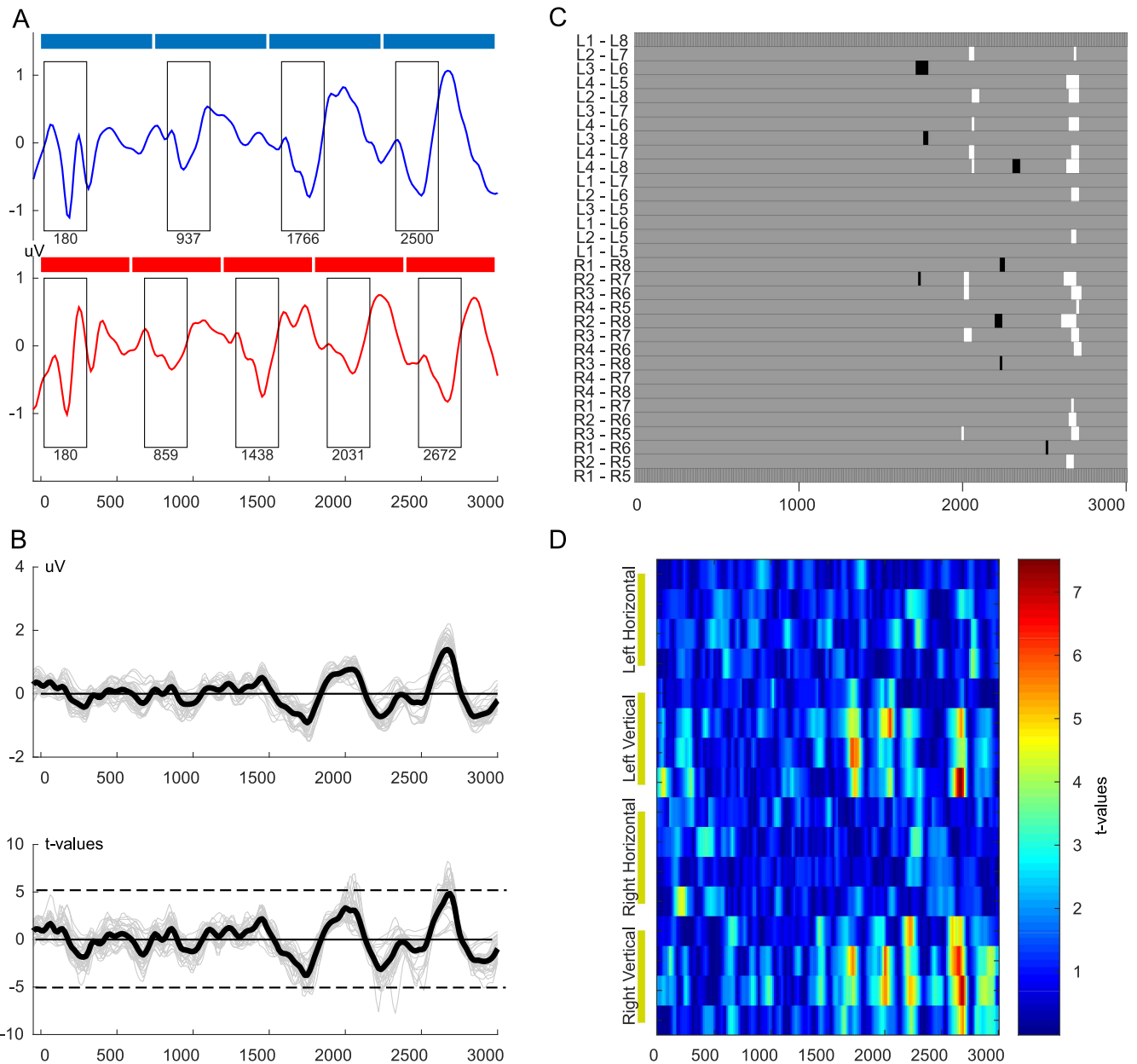


Figure 5. (A) Grand average ERP of the cEEGrid electrodes (mean of R3–R6 and L3–L6) for the attend-left (blue) and attend-right (red) condition. The horizontal bars in blue (left sound stream) and red (right sound stream) indicate the sound onsets and sound durations. For each tone in the attended stream the onset responses can be seen (boxes), the numbers indicate the respective peak latencies. Based on the latency of the first N1 (180 ms) the peaks should occur at 930, 1680 and 2430 ms for the attend-left conditions, and at 780, 1380, 1980 and 2580 ms for the attend-right condition. The observed latencies occur approximately 70 ms later. (B) Top: butterfly plot illustrating difference waves between attend-left and attend-right. Each waveform (gray) represents one of the 32 cEEGrid vertically oriented channel pairs. The black line shows the average difference wave for all electrodes. Bottom: butterfly plot of the temporal evolution of the t -values (attend left-attend right) for all electrodes (gray) and their average (black) according to the t_{\max} permutation test. The horizontal dashed line represents the critical t -score FWER corrected for the number of channels and time points (critical t -value: ± 5.30). A t -score more extreme than the critical t -scores indicates a significant difference between the conditions for that electrode. (C) Raster diagram illustrating the same results for each electrode and time bin; each row represents one electrode, each column represents one time bin. White and black rectangles indicate electrodes/time points in which the ERP differences are significant, more positive or negative respectively. Gray rectangles indicate electrodes/time points at which no significant differences were found. (D) Raster diagram illustrating the t -scores for horizontally and vertically oriented channels for the left and the right cEEGrid, rows represent electrodes, columns represent time bins (critical t -value, ± 5.10 , FWER corrected for multiple comparisons). From top to bottom (L2–L3, L1–L4, L8–L5, L7–L6, L1–L8, L2–L7, L3–L6, L4–L5 and R2–R3, R1–R4, R8–R5, R7–R6, R1–R8, R2–R7, R3–R6, R4–R5).

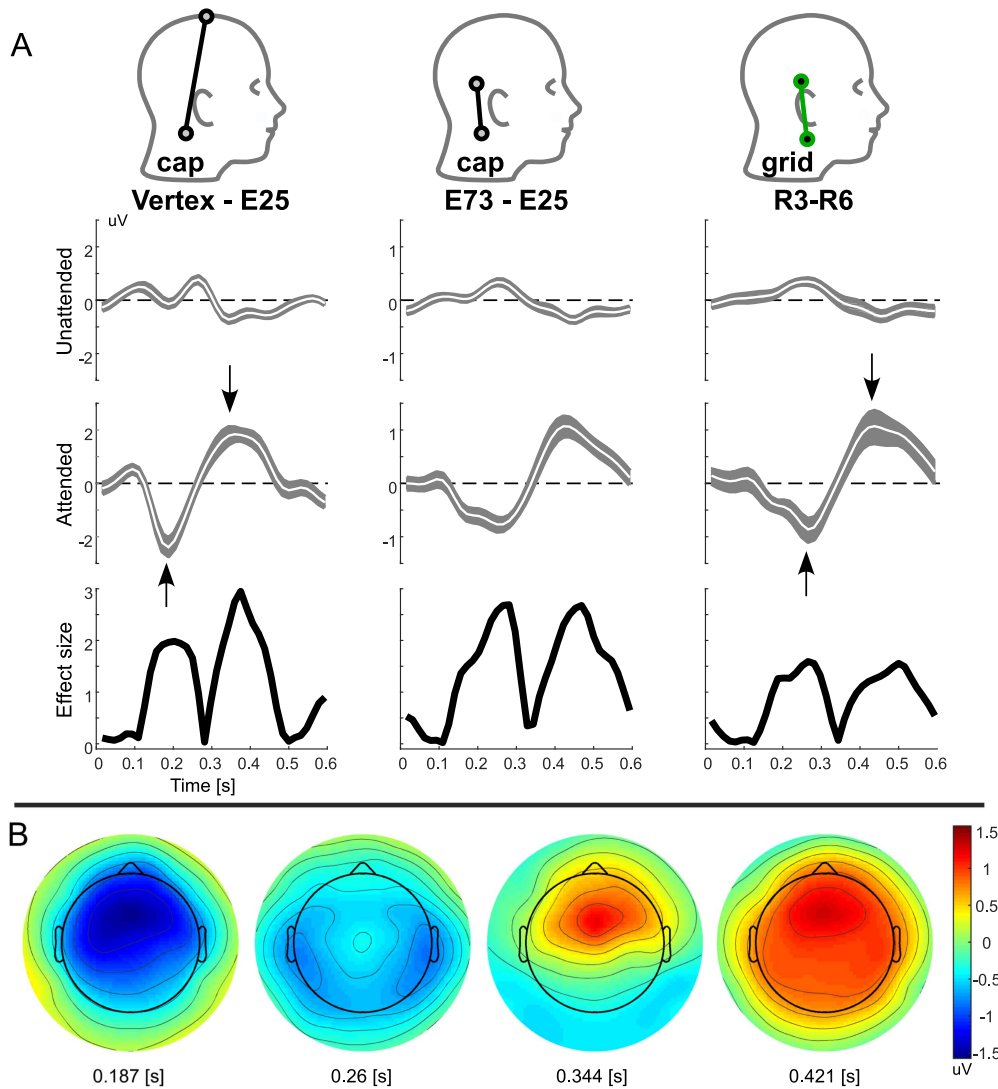


Figure 6. (A) Average ERP waveforms (shown in white) for bipolar channels of the cap (column 1 and 2 and the cEEGrid (column 3), for unattended tones (1st row) and attended (2nd row). The shaded gray areas show the standard error of the mean. Note the values on the y-axis are different for the first electrode pair. The heads indicate the position of the respective recording electrodes (black and green circles). The effect size over time is given as Hedges' *g* (bottom row, absolute values). (B) Topographic maps of the attended condition for four time points, corresponding to the first negative (0.187 s) and second positive (0.344 s) peak of the vertex electrode and the first negative (0.26 s) and second positive (0.421 s) peak of the cEEGrid electrode as indicated by the errors. It is evident that several sub-processes with different topographies occur over time. The different electrode configurations (i.e. different orientations) are more or less sensitive to the different sub-process. The vertex electrode is sensitive to the tangential source, while the cEEGrid electrodes are more sensitive to the radial than the tangential source.

horizontally oriented channels (critical *t*-value, ± 5.10 , FWER corrected for multiple comparisons).

For both systems we see N1 responses to the tone onsets of the attended sound stream. The observed differences between conditions are significantly different and increase over time.

The analysis of the individual responses to attended and unattended tones shows clear differences. For the attended tones there is a P1–N1–P2 pattern for cap (vertex electrode) and the cEEGrid electrodes (figure 6(A)). The amplitude of the vertex electrode is roughly twice as large as the amplitude observed at the ear. There is a clear latency shift of the N1 between the vertex electrode and the cEEGrid: the vertex electrode shows a peak at around 190 ms, whereas the

cEEGrid electrode shows a peak at around 250 ms. Furthermore, for the cEEGrid a double peak pattern of the N1 is visible which is absent for the vertex electrode. When comparing the cEEGrid to a cap channel pair that has a comparable inter-electrode distance, location and orientation (figure 6(A), middle column) these differences disappear to a large extent. The effect size (Hedges' *g*) over time was similar for cap-EEG and cEEGrid, both in its temporal evolution as well as in its magnitude, and can be considered as a very strong effect (> 1). The topographic representation of the ERP of the attended tones (figure 6(B)) shows a central negativity at the time of the first negative peak observed at the vertex electrode (187 ms). The observed activity pattern corresponds to what has been described as the tangential dipole source of

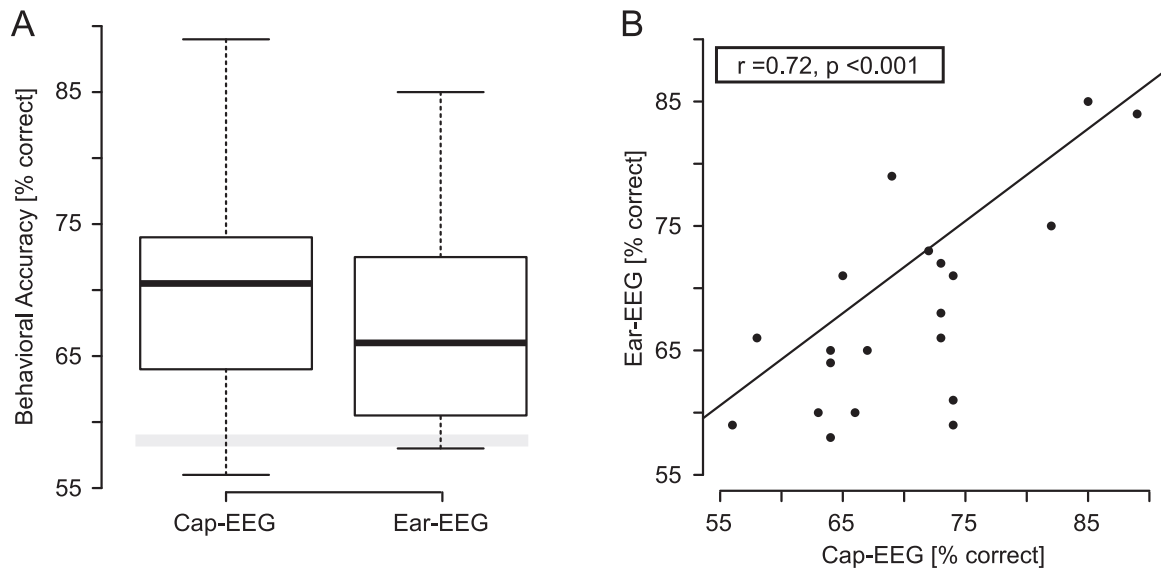


Figure 7. (A) Boxplot of the classification accuracies for cap-EEG and ear-EEG. The gray horizontal bar indicates the significant chance level. (B) Scatter plot of the individual classification results for cap-EEG and cEEGrid-EEG showing a significant positive correlation.

the N1 in the literature (Näätänen and Picton 1987). The bilateral negativity at the time of the negative peak observed for the cEEGrid (260 ms) is in accordance to the radial dipole source of the N1. The negativity is followed by the fronto-central positivity of the P2. The vertex electrode (referenced to E25) is almost ideally oriented to be sensitive to the tangential component of the N1. While the orientation of the cEEGrid electrode appears to make it sensitive to both sources (to different degrees).

Classification results

The single trial classification results revealed above chance classification for cap-EEG (median 70%, range 56%–89%) and cEEGrid-EEG (median 66%, range 57%–85%) data (figure 7(A)). For the cap-EEG data 17 out of 20 participants showed an above chance classification accuracy, while for cEEGrid-EEG data 16 out of 20 participants performed above chance. There was no significant difference between the classification accuracies of cap-EEG and cEEGrid-EEG data (Wilcoxon signed rank test: $W = 1, Z = -1.4777, p = 0.145, r_{\text{equivalent}} = 0.338$). Instead, the classification accuracies between cap-EEG and cEEGrid-EEG were significantly correlated, as illustrated in figure 7(B) ($r = 0.7127, p < 0.001$). There was no significant difference in the classification accuracy of the attend-left and the attend-right trials, neither for the cap-EEG ($W = 1, Z = -0.0374, p = 0.9782, r_{\text{equivalent}} = 0.006$) nor the cEEGrid-EEG data ($W = 1, Z = -0.5791, p = 0.5766, r_{\text{equivalent}} = 0.135$).

Evaluation of right ear-EEG and left ear-EEG signals. To explore whether electrodes at one ear would be sufficient for classification, the classification was done either only with right ear cEEGrid or the left ear cEEGrid. The median classification accuracy was 64% (range 48%–80%) for the left and 63% (range 53%–89%) for the right channels. For both

sides 14 out of the 20 participants showed an above chance classification accuracy. Overall there was no significant difference between the left and right side electrodes nor their combination (Friedman rank sum test, $\chi^2(2) = 3.5342, p = 0.1708, r_{\text{equivalent}} = 0.75$). On an individual basis there was a difference of 7.5% between the left and the right grid showing that for the majority of the participants one grid was better than the other.

Influence of distance and angle on the single channel classification accuracy. There was a significant relationship (Pearson's product moment correlation: $t(54) = 11.34, p < 0.001, r_{\text{equivalent}} = 0.839$) between the inter-electrode distance of the electrodes comprising a bipolar channel and classification accuracy: the larger the inter-electrode distance the higher the classification accuracy was (figure 8(A)). The median accuracy was 53% (range 51%–60%) for the first bin (1.9 cm) and 61% (range 59%–64%) for the last bin 6.9 cm. The subsequent evaluation of the angle differences within each distance bin suggested that the classification accuracy of channels with a more vertical orientation may be higher compared to channels with a more horizontal orientation (figure 8(B)).

Discussion

We provide in this study further evidence that multi-channel around the ear-EEG acquisition with the cEEGrid technology allows to record meaningful neural signals (Debener *et al* 2015). Accordingly the present study adds to the existing literature comparing ear-centered EEG with classical EEG setups (e.g., Mikkelsen *et al* 2015). The direct comparison of a full cap-EEG system with around-the-ear electrodes revealed a strong overlap in performance between both. We could replicate the results on selective auditory attention

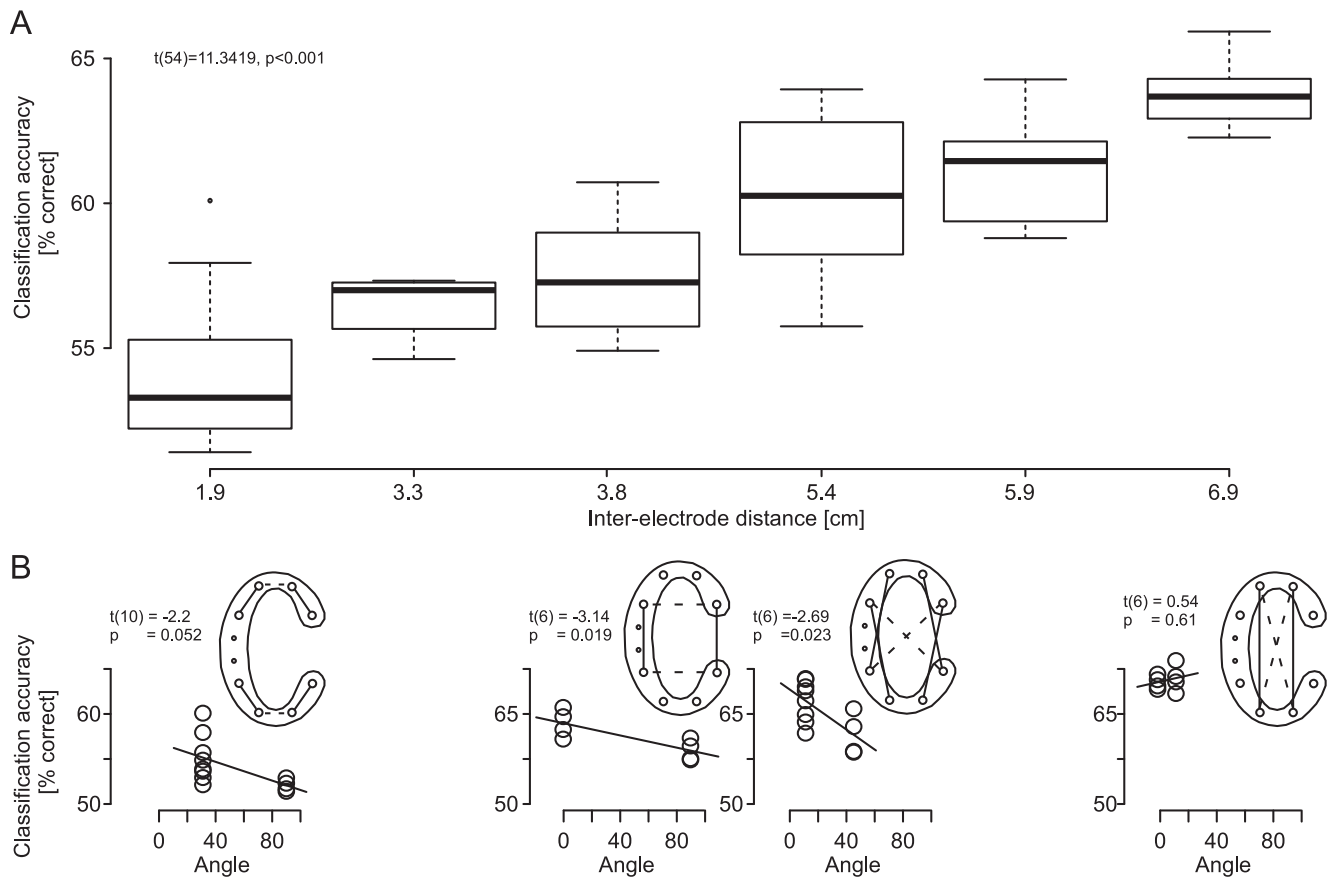


Figure 8. (A) Single channel single-trial classification accuracy for data binned into six inter-electrode distances. The horizontal bar in each boxplot indicates the median accuracy of all channels that belong to a particular bin. (B) Single channel classification accuracy as a function of the inter-electrode angle per distance bin, each circle represent a channel pair with the respective inter-electrode angle. The cEEGrids (shown for the right side, the left side is mirror reversed) indicate the locations of the respective channels, the solid lines indicate the smaller angles (left side of the plots), and the dashed lines indicate larger angles (right) side of the plot; a vertical line corresponds to 0°, a horizontal line to 90°. Note that for the 3.3 and the 5.9 cm bin, there is no variation in angle among the corresponding channels. The presented *t* and *p* values are based on Pearson’s product-moment correlations.

reported previously (Choi *et al* 2013) using the cap-EEG setup and found very comparable results for cEEGrid-EEG signals. For both electrode setups we confirmed that the ERPs followed the temporal pattern of the attended sound stream, as expected. The permutation statistics showed significant difference between the attend-left and attend-right condition both for the cap and the cEEGrid. For both setups the differences occur primarily in the second part of the stimulus. The majority of cap electrodes that show significant differences between conditions are located over the left and right temporal areas in a bilateral pattern. Clear ERP differences for attended and unattended tones were present, and effect sizes were very large for both setups.

The latency difference of the N1 peak observed for the cEEGrid compared to the vertex electrode of the cap can be explained with the position and angulation of the cEEGrid electrodes. The auditory N1 wave has several sub-components that originate from different parts of the temporal cortex (Näätänen and Picton 1987, Picton *et al* 1999). These components differ in their location of origin and their temporal evolution and therefore project differently onto the scalp. Näätänen and Picton (1987) describe a tangential and a radial

dipole source (also referred to as *T* complex (Wolpaw and Penry 1975)) that contribute to the N1. The tangential portion peaks earlier than the radial source by around 40–50 ms, which fits with the latency differences we have observed here. The vertex electrode of the cap (referenced to E25) is almost ideally oriented to capture the tangential portion of the N1. The cEEGrid electrodes however are more vertically oriented (parallel to the side of the head), as a consequence they capture both the tangential (but reduced in amplitude) as well as the radial source. Interestingly, both sub-components show clear differences between the attended and unattended tones.

Furthermore, we observed that the N1 peak to the stimulus onset appears earlier than the N1 peak to the remaining tones. This is the case for cap and for the cEEGrid, and is also observable in the waveform reported by Choi (see figure 4, Choi *et al* 2013). While the stimulus onset is a very salient event, as all streams start simultaneously, the remaining tones require attention to separate the attended tones from the unattended tones. It is therefore possible that the N1 in response to the first tone is generated differently than the N1 of the following tones and therefore shows a different temporal profile (Sanmiguel *et al* 2013).

The classification performance for both systems was above chance level for the majority of the participants (16 out of 20 cEEGrid, 17 out of 20 for the Cap). The median classification accuracy of 70% that we found with the cap-EEG is in line with the 71% as reported by Choi *et al* (2013). The classification accuracy between cap-EEG and cEEGrid-EEG was not significantly different. The high correlation between the classification performance achieved with the cap-EEG and the cEEGrid-EEG are additional evidence that comparable processes are captured with both systems. Interestingly, the classification analysis using only one cEEGrid (either left or right) showed that there is no significant loss in classification accuracy. However, for most participants one of the sides led to considerable higher classification results compared to the other. Future work is required to determine the test-retest reliability of this effect, which would be important for an individualized application, such as a BCI-controlled hearing aid steering. In any case, this finding suggests that a single cEEGrid may be sufficient for decoding auditory attention. However, note that while the classification accuracy we achieved was significantly above chance for both cap-EEG and cEEGrid-EEG data and reached for some participants a reasonable level of 85% and above, overall classification performance with a median accuracy of 70% (cap-EEG) and 67% (cEEGrid-EEG) is not sufficient for many BCI applications. Most auditory BCI paradigms have modest classification rates and lower transfer rates than what can be achieved in the visual sensory modality. However, future passive BCI applications (Kothe and Zander 2011) may demonstrate a benefit even for low-accuracy systems.

The core design idea of the cEEGrid was to collect multi-channel EEG signals from around the ear, enabling the selection of individual bipolar channels with different orientations. In the present study we found an effect of inter-electrode distance and angle on single channel classification accuracy. Classification accuracy was highest for channels that are relatively distant from each other and oriented vertically, as expected. Whereas the distribution of the electrodes on the cEEGrid does not allow for the analysis of distance and angle information independently, since the sampling of the distance-angle subspace is suboptimal, our results indicate that both factors play a role. The exact influence of distance and angle depends probably on the relative location of the cEEGrid to the location and orientation of a neural source of interest as well, an issue that requires further evaluation. However, ear-centered EEG approaches should be aware of this phenomenon.

When relating the cEEGrid with other ear-EEG solutions (e.g. Kidmose *et al* 2012, Bleichner *et al* 2015) that have electrodes in the outer ear canal and the concha, one should be aware of a number of factors. The electrode arrangement of the cEEGrid is more or less constrained to a plane parallel to the side of the head (2D), but provides large inter-electrode distances, and can sample different orientations. Electrodes placed in the ear however can span a 3D space, but with a much smaller inter-electrode distance, generally resulting in a much reduced signal amplitude. Based on our findings concerning the sensitivity of the cEEGrid to the later aspects of

the N1 we speculate that an electrode in the ear canal, referenced to an above ear electrode might be optimally oriented to capture the radial component of the late N1. The ideal orientation of electrodes that comprise a bipolar pair to record from a given EEG source will be a future research question.

Evidently, a small number of electrodes in or around the ear cannot be a substitute for a high-density EEG setup. However, for many EEG applications a small number of electrodes suffices (Lau 2012) and is even desirable when it comes to ease of use and user comfort (Krusienski *et al* 2008, Askamp and van Putten 2014, Wascher *et al* 2014). One strength of the behind-the-ear cEEGrid EEG approach is, that it allows for unobtrusive and concealed EEG acquisition. In combination with a small amplifier and a smartphone based recording system (Debener *et al* 2015) this enables out-of-the-laboratory EEG recordings over extended periods of times and provides therefore the means to study the relationship between brain and behavior in more naturalistic settings. A further advantage of the around the ear setup is the fast electrode placement and the easy electrode removal after the recording that make it an interesting candidate for applications such as BCI or continuous EEG monitoring. Future studies have to investigate the motion tolerance of this recording setup which would be a prerequisite for EEG measurements in daily life applications. Moreover, an online smartphone-operated BCI application, used in daily life settings, would be needed before ear-EEG could be merged with hearing aid technology to adjust devices to user states and needs.

Conclusion

We replicate the single-trial selective auditory attention results of Choi *et al* (2013) using a classical EEG cap setup. Moreover, we demonstrate that around-the-ear, cEEGrid based EEG acquisition results in similar system performance. The overall task-induced auditory attention effects seem to be similarly well captured by cEEGrid-EEG and cap-EEG, whereas the cEEGrid seems to be especially sensitive to the later components of the N1. For auditory attention monitoring, concealed behind-the-ear EEG recordings can be an alternative to classical cap EEG acquisition.

Acknowledgments

We thank Reiner Emkes for his technical support, and Jeremy Thorne and Joost Meekes for their valuable comments. We thank Twente Medical Systems International BV, Oldenzaal, The Netherlands, for sharing knowledge and supporting the design and production of the cEEGrid. We are grateful to mBrainTrain, Belgrade, Serbia, for development of the SMARTING amplifier and excellent software support. This research was funded by Task Group 7 'BCI for Hearing Aids' and other funds from the DFG Cluster of Excellence 1077 'Hearing4all', Oldenburg, Germany.

References

- Askamp J and van Putten M J A M 2014 Mobile EEG in epilepsy *Int. J. Psychophysiol.* **91** 30–5
- Bleichner M G, Lundbeck M, Selisky M, Minow F, Jager M, Emkes R, Debener S and De Vos M 2015 Exploring miniaturized EEG electrodes for brain–computer interfaces. An EEG you do not see? *Physiol. Rep.* **3** e12362
- Brainard D H 1997 The psychophysics toolbox *Spat. Vis.* **10** 433–6
- Choi I, Rajaram S, Varghese L A and Shinn-Cunningham B G 2013 Quantifying attentional modulation of auditory-evoked cortical responses from single-trial electroencephalography *Front. Hum. Neurosci.* **7** 115
- de Vos M and Debener S 2013 Mobile EEG: towards brain activity monitoring during natural action and cognition *Int. J. Psychophysiol.* **91** 1–2
- De Vos M, Kroesen M, Emkes R and Debener S 2014 P300 speller BCI with a mobile EEG system: comparison to a traditional amplifier *J. Neural Eng.* **11** 36008
- Debener S, Emkes R, De Vos M and Bleichner M 2015 Unobtrusive ambulatory EEG using a smartphone and flexible printed electrodes around the ear *Sci. Rep.* **5** 16743
- Debener S, Minow F, Emkes R, ras G, K, Vos M, de Vos M and Gandras K 2012 How about taking a low-cost, small, and wireless EEG for a walk? *Psychophysiology* **49** 1617–21
- Gramann K, Gwin J T, Ferris D P, Oie K, Jung T P, Lin C T, Liao L D and Makeig S 2011 Cognition in action: imaging brain/body dynamics in mobile humans *Rev. Neurosci.* **22** 593–608
- Gramann K, Jung T P, Ferris D P, Lin C T and Makeig S 2014 Toward a new cognitive neuroscience: modeling natural brain dynamics *Front. Hum. Neurosci.* **8** 444
- Groppe D M, Urbach T P and Kutas M 2011 Mass univariate analysis of event-related brain potentials/fields: I. A critical tutorial review *Psychophysiology* **48** 1711–25
- Hine J and Debener S 2007 Late auditory evoked potentials asymmetry revisited *Clin. Neurophysiol.* **118** 1274–85
- Kidmose P, Looney D, Ungstrup M, Rank M and Mandic D 2013 A study of evoked potentials from ear-EEG *IEEE Trans. Biomed. Eng.* **60** 2824–30
- Kidmose P P, Park C C, Ungstrup M M, Rank M M, Rosenkranz K K, Mandic D D and Looney D D 2012 The In-the-Ear recording concept: user-centered and wearable brain monitoring *IEEE Pulse* **3** 32–42
- Kleiner M, Brainard D H, Pelli D G, Broussard C, Wolf T and Niehorster D 2007 What's new in Psychtoolbox-3? *Perception* **36** S14
- Kothe C and Zander T 2011 Towards passive brain–computer interfaces: applying brain–computer interface technology to human–machine systems in general *J. Neural Eng.* **8** 25005
- Krusienski D J, Sellers E W, McFarland D J, Vaughan T M and Wolpaw J R 2008 Toward enhanced P300 speller performance *J. Neurosci. Methods* **167** 15–21
- Lau T M 2012 How many electrodes are really needed for EEG-based mobile brain imaging? *J. Behav. Brain Sci.* **02** 387–93
- Lee J H, Lee S M, Byeon H J, Hong J S, Park K S and Lee S-H 2014 CNT/PDMS-based canal-typed ear electrodes for inconspicuous EEG recording *J. Neural Eng.* **11** 46014
- Lin Y-P, Wang Y and Jung T-P 2014 Assessing the feasibility of online SSVEP decoding in human walking using a consumer EEG headset *J. Neuroeng. Rehabil.* **11** 119
- Looney D, Park C, Kidmose P, Rank M L, Ungstrup M, Rosenkranz K and Mandic D P 2011 An in-the-ear platform for recording electroencephalogram *Conf. Proc. IEEE Eng. Med. Bio. Soc., EMBS* 6882–5
- Mikkelsen K B, Kappel S L, Mandic D P and Kidmose P 2015 EEG recorded from the ear: characterizing the ear-EEG method *Front. Neurosci.* **9**
- Müllensiefen D, Gingras B, Musil J and Stewart L 2014 The musicality of non-musicians: an index for assessing musical sophistication in the general population *PLoS One* **9**
- Müller-Putz G R, Scherer R, Brunner C, Leeb R and Pfurtscheller G 2008 Better than random? A closer look on BCI results *Int. J. Bioelectromagn.* **10** 52–5
- Näätänen R and Picton T 1987 The N1 wave of the human electric and magnetic response to sound: a review and an analysis of the component structure *Psychophysiology* **24** 375–425
- Norton J J S et al 2015 Soft, curved electrode systems capable of integration on the auricle as a persistent brain–computer interface *Proc. Natl Acad. Sci.* **112** 201424875
- Nunez P L and Srinivasan R 2006 *Electric Fields of the Brain: The Neurophysics of EEG* 2nd edn (New York: Oxford University Press) (doi:10.1093/acprof:oso/9780195050386.001.0001)
- Pelli D G 1997 The videotoolbox software for visual psychophysics: transforming numbers into movies *Spat. Vis.* **10** 437–42
- Picton T, Alain C, Woods D L, John M S, Scherg M, Valdes-Sosa P, Bosch-Bayard J and Trujillo N J 1999 Intracerebral sources of human auditory-evoked potentials *Audiol. Neuro-Otol.* **4** 64–79
- 2013 R: A language and environment for statistical computing. R Foundation for Statistical Computing, Vienna, Austria <http://R-project.org/> R Found. Stat. Comput. Vienna, Austria
- Rosenthal R and Rubin D B 2003 r equivalent: a simple effect size indicator *Psychol. Methods* **8** 492–6
- Sanmiguel I, Todd J and Schröger E 2013 Sensory suppression effects to self-initiated sounds reflect the attenuation of the unspecific N1 component of the auditory ERP *Psychophysiology* **50** 334–43
- Schaal N K, Bauer A-K R and Müllensiefen D 2014 Der Gold-MSI: replikation und validierung eines fragebogeninstrumentes zur Messung musikalischer erfahrungheit anhand einer deutschen stichprobe *Music. Sci.* **18** 423–47
- Wascher E, Heppner H and Hoffmann S 2014 Towards the measurement of event-related EEG activity in real-life working environments *Int. J. Psychophysiol.* **91** 3–9
- Wolpaw J R and Penry J K 1975 A temporal component of the auditory evoked response *Electroencephalogr. Clin. Neurophysiol.* **39** 609–20